ON THE TERRESTRIAL DETECTION OF FRAME-DRAGGING

Matthew P. Cartmell,
Department of Mechanical & Aerospace Engineering
University of Strathclyde,
Glasgow,
Scotland, UK

2nd Conference on Nonlinearity, Belgrade, Serbia

The Foucault Pendulum – a possible measurement instrument

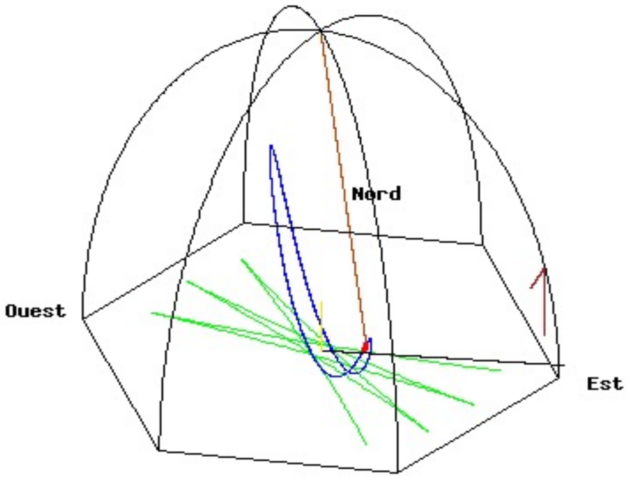

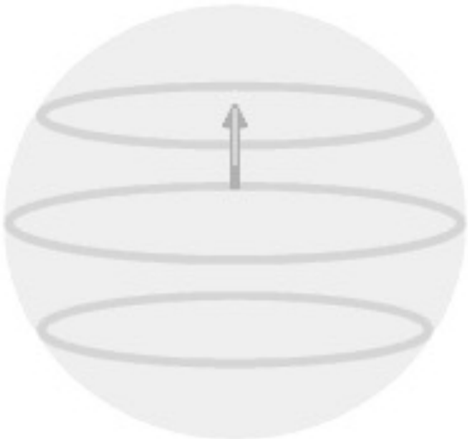

[both gifs courtesy of Wikipedia, October 2021]

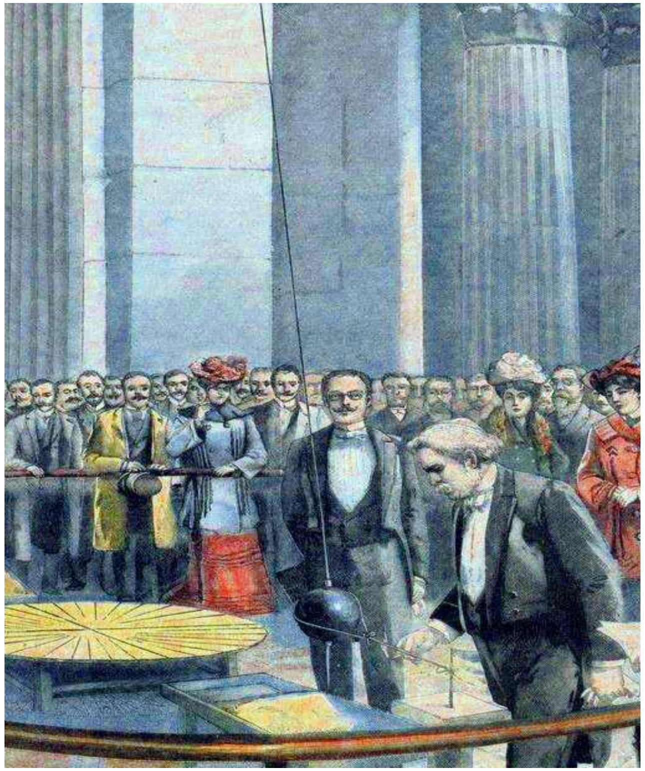

[source – Wikipedia (*Le Petit Parisien* November 2, 1902, 50th anniversary of the experiment of Léon Foucault demonstrating the rotation of Earth]

Léon Foucault demonstrated his famous 67 metre pendulum with a 22 kg bob mass at the Panthéon in Paris in 1851. It has since become one of the fundamental experiments of physics. The period of Foucault's 67 m pendulum was 16.5 s and the latitude of the Panthéon is $48° \, 52'$ N. The plane of oscillation there makes one rotation in: $\frac{23h \; 56m \; 4s}{sin\phi} \sim 31$ hours 50 mins. So it's precession rate at that location is $11.3°$/hour. A 'pendulum day' is therefore dependent on the latitude of the location.

Foucault pendulum location

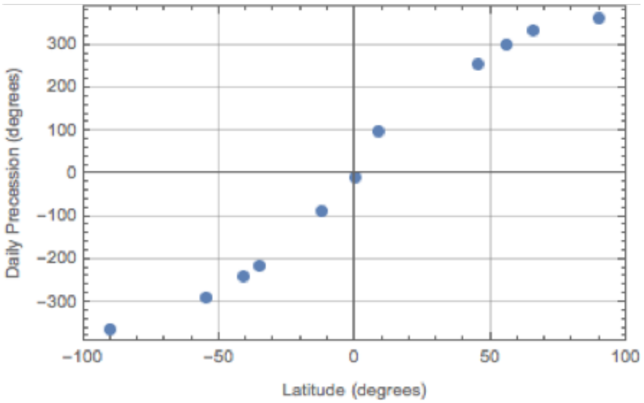

Predicted daily FP precession against latitude

Linear drive (top end)

Spherical joint (top end)

Parametric excitation of the pendulum

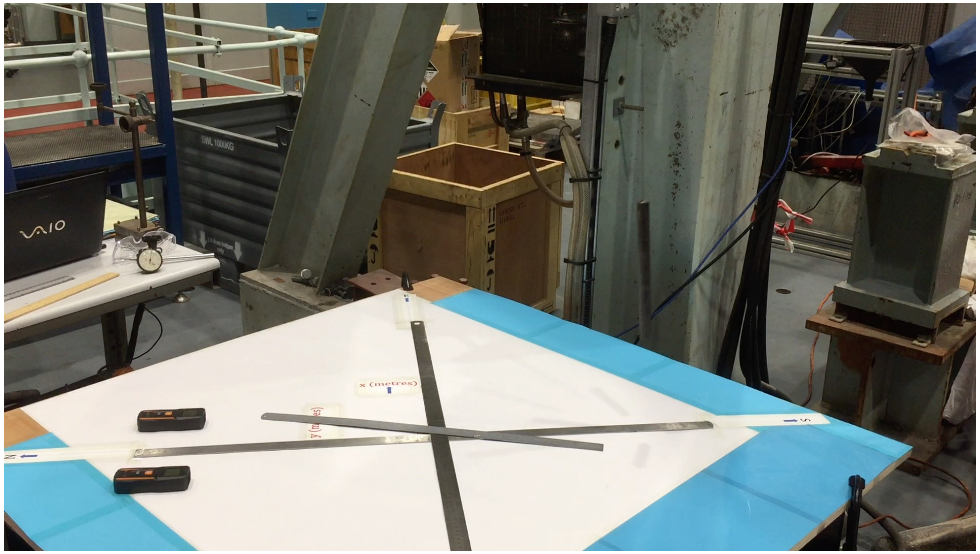

$l_0 = 4.6855$ +/- 0.0005 m. Test pendulum suspended from laboratory roof, University of Strathclyde, and driven into principal parametric resonance through length variation $l_1 = 0.001 l_0$. Tempered mild-steel wire, tungsten bob.

Snapshots of geographical location data

Location	Latitude (°/rad)	Radius of Earth (km)	Acceleration due to Gravity (m/s²)	Height above Sea Level (m)
North Pole	90/1.5707	6357.00	9.8320	0.1
Luleå	65.585/1.144	6360.43	9.8235	6
Glasgow	55.865/0.9750	6363.18	9.8156	40
Grenoble	45.166/0.7882	6367.64	9.8057	213
Addis Ababa	8.98/0.1567	6377.62	9.7743	2355
Quito	-0.1807/-0.0031	6378.14	9.7715	2850
Darwin	-12.463/-0.2175	6377.15	9.7826	27.8
Adelaide	-34.928/-0.6096	6371.16	9.7971	50
Wellington	-41.28/-0.7205	6368.87	9.8027	31
Ushuaia	-54.802/-0.9565	6363.89	9.8145	195
South Pole	-90/-1.5707	6357.00	9.8320	2835

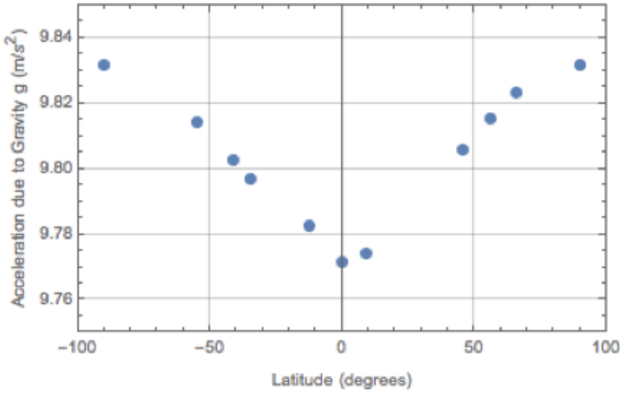

g against latitude

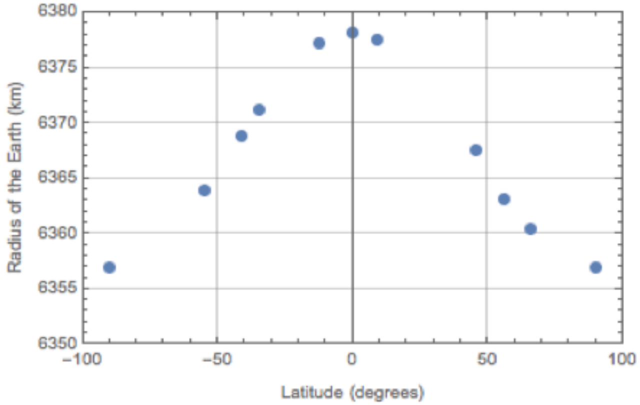

Radius of Earth against latitude - oblateness

Modelling – equations of motion in Earth centred system:

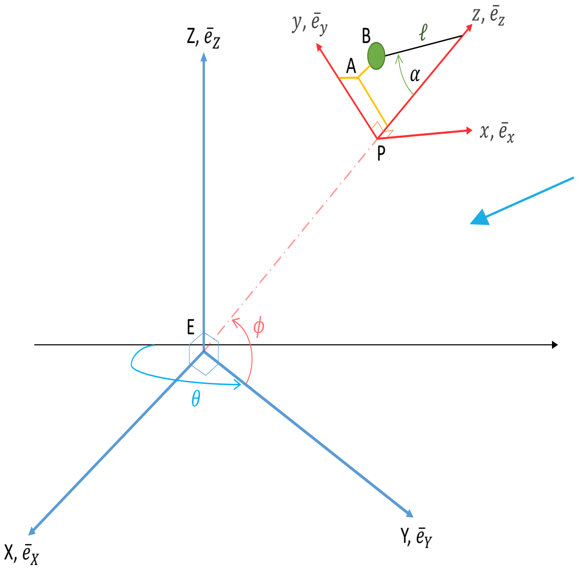

Earth-fixed frame – pendulum at latitude ϕ, location *p*

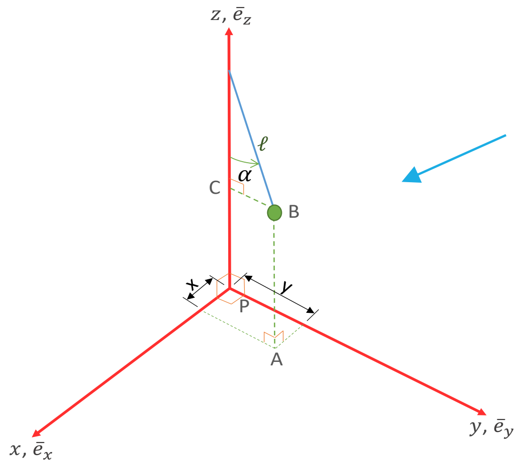

Local system, located at *p*, coordinates *x* and *y*

$$\ddot{x} + \eta|\dot{x}|\dot{x} - 2\dot{y}\Omega sin\phi - x\Omega^2 + \frac{gx}{l\sqrt{1-\frac{x^2+y^2}{l^2}}} = 0$$

$$\ddot{y} + \eta|\dot{y}|\dot{y} + 2\dot{x}\Omega sin\phi - y\Omega^2 sin^2\phi + r\Omega^2 sin\phi cos\phi + \frac{gy}{l\sqrt{1-\frac{x^2+y^2}{l^2}}} = 0$$

[Cartmell, Faller, Lockerbie, Handous, 2020]

A new pendulum design – no excitation and then parametrically excited

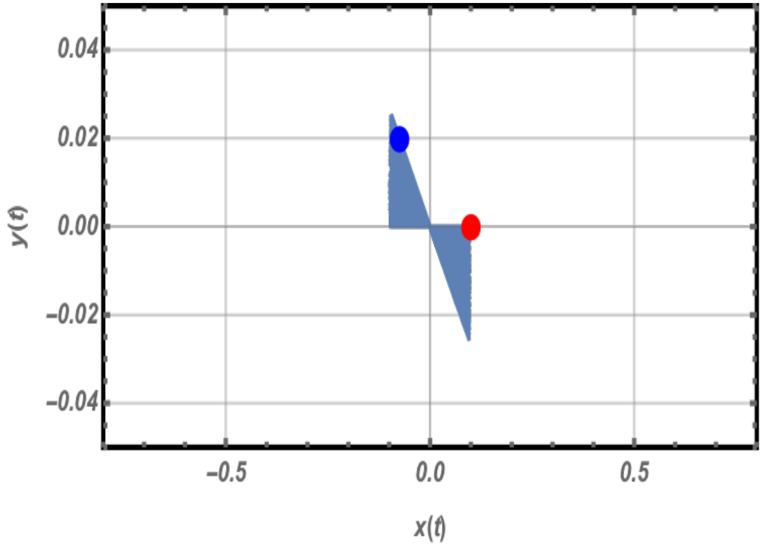

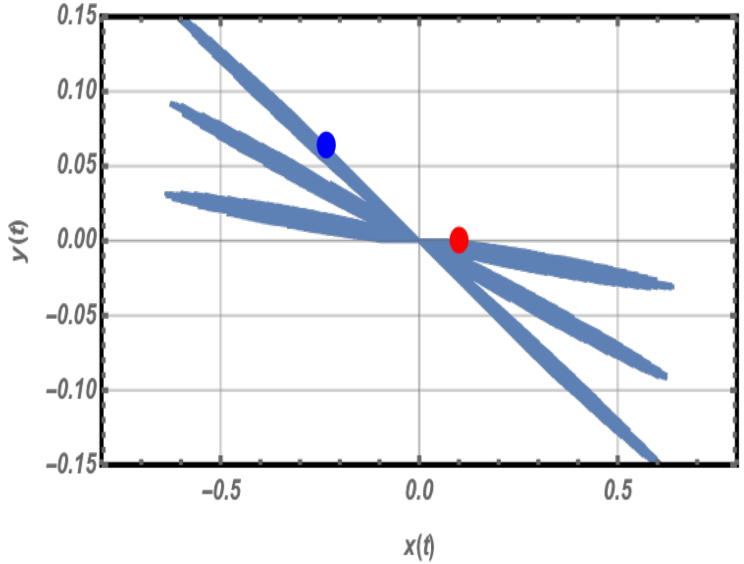

Pendulum response over 1 hour at the North Pole for no parametric excitation, $l_1 = 0$ (*left*) and for parametric excitation, $l_1 = 0.040\, m$ (*right*). Red dots: displ. ICs $(x_0, y_0) = (0.1, 0)\, m$, blue dots: end points (x_{tend}, y_{tend}), vel ICs are $\dot{x}_0 = \dot{y}_0 = 0\, m/s$. Data: $l_0 = 4\, m,\ g = 9.8320\, m/s^2,\ \Omega = 7.2921150 * 10^{-5}\ rad/s,\ \phi = 1.5705\, rad,\ r = 6357.00 * 10^3\, m,\ m = 5\, kg,\ \rho = 1.189\ kg/m^3,\ C_D = 10^{-6},\ R_{bob} = 0.0463134\, m,\ t_{end} = 3600\, s,\ \epsilon\sigma = 0.$

Displacements in metres.

Effect of increasing the displacement ICs

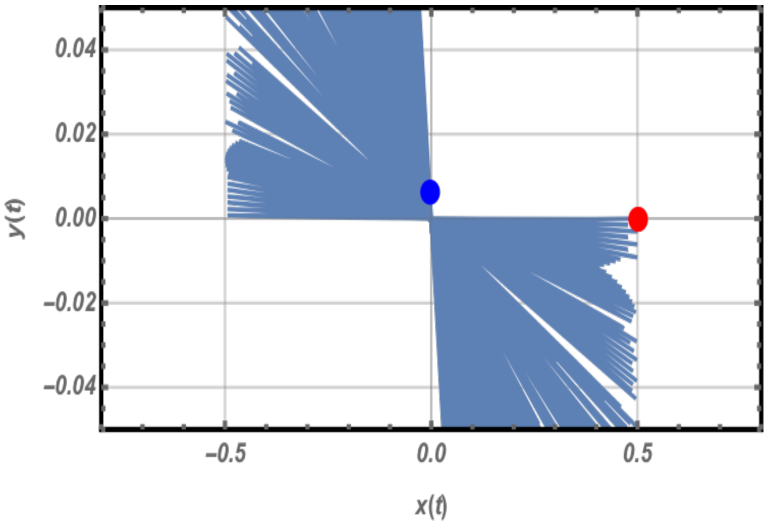

Pendulum response over 4 hours at the North Pole for no parametric excitation, same data except for $x_0 = 0.5\,m$ and $t_{end} = 14400\,s$.

PPR	**3,600 *s***	**Sidereal day**
off	15.042 º	360.029 º
on	15.027 º	359.671 º
PPR	**14,400 *s***	**Sidereal day**
off	60.016º	360.095º

Predicted precessions at the North Pole for two different integration times and parametric excitation off/on.

These numerical results suggest that the North Pole can be a benchmark location for validating the numerical integration routine, and therefore predicting the operation of the pendulum in other places. See [Cartmell, Faller, Lockerbie, and Handous, 2020] for a fuller exploration of locations.

Locating the new pendulum in Glasgow, Scotland

Glasgow is at a latitude of 55.86º N (0.975 rad N), noting that the local values for the acceleration due to gravity, g, and the radius of the Earth, r, vary from those for the North Pole, all other data maintained except where specifically indicated.

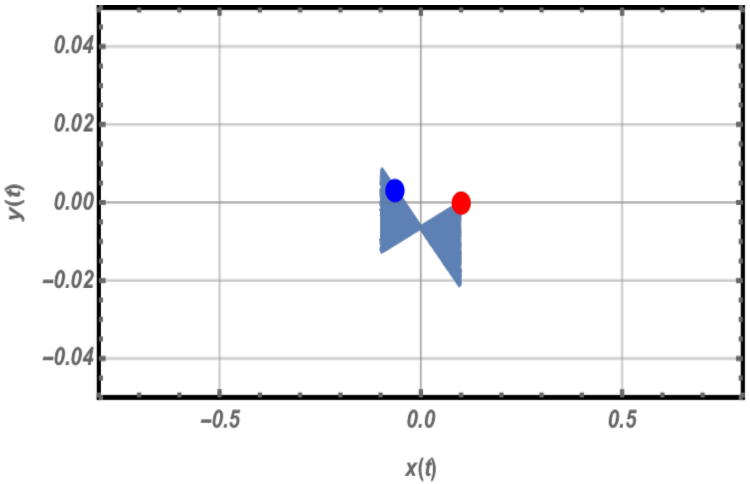

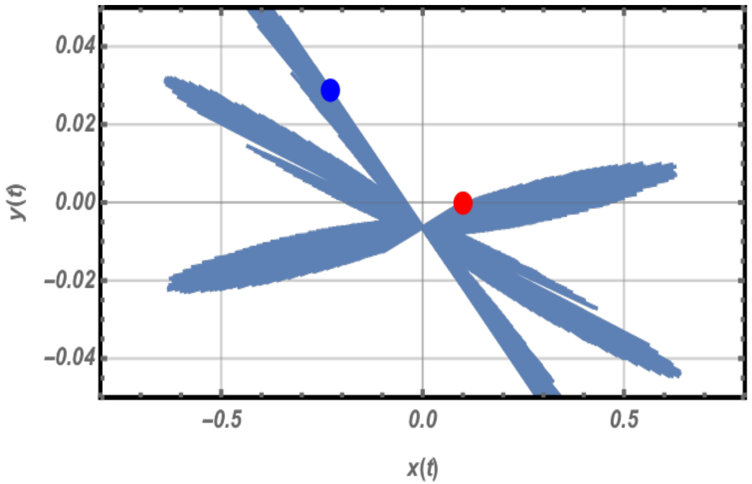

PPR	3,600 *s*	Sidereal day
off	12.420 º	297.265 º
on	12.358 º	296.503 º

Precession data for Glasgow given in the table, over 1 hour and then extrapolated over one sidereal day. The aggregated numerical error can potentially be $< 0.1\%$.

Pendulum responses over 1 hour at Glasgow for no parametric excitation, $l_1 = 0$ (*left*) and for parametric excitation, $l_1 = 0.040\, m$ (*right*). Red dots: displ. ICs $(x_0, y_0) = (0.1, 0)\, m$, blue dots: end points (x_{tend}, y_{tend}), velocity ICs are $\dot{x}_0 = \dot{y}_0 = 0\, m/s$. Data: $l_0 = 4\, m,\ g = 9.8156\, m/s^2,\ \Omega = 7.2921150 * 10^{-5}\ rad/s,\ \phi = 0.9750\, rad,\ r = 6363.18 * 10^3\, m,\ m = 5\, kg,\ \rho = 1.189\ kg/m^3,\ C_D = 10^{-6},\ R_{bob} = 0.0463134\, m,\ t_{end} = 3600\, s,\ \epsilon\sigma = 0.$

Foucault pendulum performance – a fundamental difficulty:

- A very real problem with all Foucault pendulums is the tendency for the planar motion to degenerate into ellipticity over time.
- It's associated with a frequency anisotropy effect, showing increasingly different periods of each axis of the developing elliptical response.
- This effect is triggered by structural asymmetries – much worse in shorter pendulums.
- This is why Foucault's relatively long 67 metre installation in the Panthéon operated quite successfully over time.
- So, longer Foucault pendulums are *inherently less sensitive* to ellipticity error than shorter pendulums, and we must therefore maximise pendulum length as far as possible.

- Our analyses have shown that the dependence on length for ellipticity error is proportional to $\frac{1}{l^{5/2}}$.

How do we solve this problem?

- Symmetrical design, very high-quality manufacture, and installation – very difficult to achieve perfection.
- Pippard [Pippard, 1988] suggested that parametric excitation of the length could mitigate this effect.
- Electro-mechanical mitigation measures such as electromagnetic pusher drives can be effective.

Parametric excitation is effective but very difficult to install practically. A 'pusher' is better.

Applying the pendulum - a measurement challenge

General Relativity states that inertial frames are 'influenced and dragged by the distribution and flow of mass–energy in the universe', noting the relativistic equivalence of mass and energy [Chartas, 2020].

A theory for *frame-dragging* was proposed by Hans Thirring and Josef Lense in 1918, in which inertial frames are dragged around a central rotating mass due to the effect of its gravity on the surrounding spacetime.

The rotation of the central mass twists the surrounding spacetime, and this perturbs the orbits of other masses nearby. This effect is known as Lense-Thirring precession (LT). The Earth's gravitational field is capable of generating the frame dragging effect of LT precession.

LT precession around Earth has been measured before

The GP-B and the LAGEOS/LARES satellites both provided confirmatory measurements of LT precession in LEO – but at some considerable cost …

[https://www.nasa.gov/mission_pages/gpb/]

The GP-B satellite mission

The GP-B satellite used *IM Pegasi HR 8703* as the guide star and operated on a circular polar orbit of 642 km altitude. The spin axes of GP-B's gyroscopes drifted so the Geodetic precession (due simply to the presence of the mass of Earth rather than its presence *and* its rotation) was only measured to a precision of 1.5%, which had a significant knock-on effect on the measurement of LT. GP-B measured LT to ~ 0.039 arcsecs/year, which is 10.833 x 10^{-6} °/year.

By August 2008, the LT precession had been confirmed to within 15-20% of the expected result. This took almost 50 years from planning to completion and cost US$ 750M.

The LAGEOS/ LARES satellites

The LAGEOS/LARES missions consisted of the following key goals:

- to provide an accurate measurement of the satellite's position with respect to Earth.
- to determine the planet's shape (geoid).
- to determine tectonic plate movements associated with continental drift.

LAGEOS/LARES measured the LT drag of its orbital plane to ~ 0.031 arcsecs/year, which is ~ 8.611 x 10^{-6} °/year. This was subject to error due to uncertainty in the Earth's mass distribution, and there is still some debate about the true size of the error in LAGEOS's LT measurement but it mainly derived from the low eccentricity of the LAGEOS orbits and the difficulties in eliminating Earth multipoles.

[Ciufolini et al, 2011]

[https://lageos.gsfc.nasa.gov/ & https://earth.esa.int/web/eoportal/satellite-missions/l/lares]

Gravitoelectromagnetism - GEM

Maxwell's Equations

$$\nabla.\bar{E} = \frac{\rho}{\varepsilon_0}$$

The quantity of electric field coming from a region of space is proportional to the total electric charge in that region.

$$\nabla.\bar{B} = 0$$

The magnetic field doesn't come or go but travels in a continuous loop, so a monopole can't exist in practice, according to Maxwell.

$$\nabla\times\bar{E} = -\frac{\partial\bar{B}}{\partial t}$$

The curl of the electric field equals the negative of the rate of change of the magnetic field. Changing the magnetic field alters the curl of the electric field, with the negative sign defining that they go in opposite directions. So, the curl of the electric field pushes electric charge round in a circle in the form of an electric current.

$$\nabla\times\bar{B} = \mu_0\bar{J} + \mu_0\varepsilon_0\frac{\partial\bar{E}}{\partial t}$$

The curl of the magnetic field is proportional to the current density and a changing electric field.

The GEM analysis behind LT is derived in terms of a *weak* gravitomagnetic effect on an accelerating mass (at low, non-relativistic velocities), and so this can be considered analogously with an accelerating charge producing a magnetic field, as in Maxwell's equations.

If we consider spacetime to be stationary around the Earth then this simplifying stationarity is a basis for decomposing the Kerr spacetime metric tensor $g_{\mu\nu}$ naturally into constituent parts – from which GEM then flows.

Gravitoelectromagnetism - GEM

Maxwell's equations

$$\nabla.\bar{E} = \frac{\rho}{\varepsilon_0}$$

$$\nabla.\bar{B} = 0$$

$$\nabla\times\bar{E} = -\frac{\partial\bar{B}}{\partial t}$$

$$\nabla\times\bar{B} = \mu_0\bar{J} + \mu_0\varepsilon_0\frac{\partial\bar{E}}{\partial t}$$

Gravitomagnetic equations

$$\nabla.\bar{E}_G = -4\pi G\rho_m$$

$$\nabla.\bar{H} = 0$$

$$\nabla\times\bar{E}_G = 0$$

$$\nabla\times\bar{H} = 4\left[-4\pi G\frac{\rho_m\bar{v}}{c} + \frac{1}{c}\frac{\partial\bar{E}_G}{\partial t}\right]$$

Gravity is attractive, but electromagnetism is both attractive and repulsive, so this difference leads to the minus signs in the RHS 'source terms' in the first and fourth GEM equations.

The gravitational tensor introduces the additional 4 in the fourth equation.

The space-space components from the gravitational metric tensor correspond to curved space rather than Euclidean space. As we are only interested here in the effects of the Earth's rotation on an orbiting test mass then we can neglect the curvature of space and also those terms that are not gravitometric and of the order of $(\frac{v}{c})^2$.

In the GEM analogy the electric field of Maxwell's equations $\bar{E}$ becomes the gravitoelectric field $\bar{E}_G$ and the magnetic field of Maxwell's equations $\bar{B}$ becomes the gravitomagnetic field $\bar{H}$. The electric charge density ρ becomes the mass density ρ_m. The charge current density $\bar{J}$ becomes the mass current density defined by $G\rho_m\bar{v}$, where G is Newton's gravitational constant and $\bar{v}$ is the velocity of the source mass.

Gravitoelectromagnetism - GEM

The conventional magnetic moment $\bar{\mu}$ of Maxwellian electrodynamics creates a dipole magnetic field:

$$\bar{B} = \frac{3\bar{n}(\bar{n} \cdot \bar{\mu}) - \bar{\mu}}{r^3}$$

So, inserting $\bar{\mu}_G$ instead of μ leads to an alternative form which now represents the Earth's dipolar gravitomagnetic field:

$$\bar{H} = \frac{2G}{c}\left[\frac{\bar{S} - 3\bar{n}(\bar{n} \cdot \bar{S})}{r^3}\right]$$

The abstract angular momentum for the large rotating body $\bar{S}$ can be replaced by the angular momentum specific to the Earth, defined as $\bar{L'}$ so we state the Earth's angular velocity as,

$$\bar{\Omega} = \frac{2G}{c^2 r^3}\bar{L'}$$

Therefore, the gravitomagnetic field can now be restated in terms of the Earth's angular velocity, where $\bar{S} \equiv \bar{L'}$, noting that the GF is divided by the velocity of light,

$$\frac{\bar{H}}{c} = \bar{\Omega} - 3\bar{n}(\bar{\Omega} \cdot \bar{n})$$

In order to proceed to LT we need to revert to explicit angular momentum of the Earth, and then to rearrange to get the gravitomagnetic field in terms of fundamental quantities and in the conventional form, as follows,

$$\bar{H} = \frac{4G}{c}\left[\frac{\bar{L'}r^2 - 3\bar{r}(\bar{L'} \cdot \bar{r})}{2r^5}\right]$$

Gravitoelectromagnetism - GEM

Before we complete the analysis for LT precession we state the general expression for the spin precession rate for LT from the Schiff formula statement of LT, which is,

$$\bar{\Omega}_{Tot} = \bar{\Omega}_{Th} + \bar{\Omega}_{Geo} + \bar{\Omega}_{LT}$$

where $\bar{\Omega}_{Tot}$ is the total angular velocity measured, assuming an orbital test mass. The right-hand side terms are the Thomas precession $\bar{\Omega}_{Th}$, the geodetic precession $\bar{\Omega}_{Geo}$, and the LT precession $\bar{\Omega}_{LT}$. Concentrating on the LT precession, and averaging over fast orbital motions we find that LT is directly equal to,

$$\bar{\Omega}_{LT} = \frac{H}{2c}$$

and so for a closely orbiting body we obtain the following for the averaged gravitomagnetic field at the poles,

$$\bar{H}_{poles} = \frac{4G}{c}\frac{\bar{L}'}{r^3}$$

and if we now move from a general closely orbiting body **to a specific terrestrial location where there is a body elevated at *h* from the surface of the Earth (therefore at altitude *R*, where $\boldsymbol{R} = \boldsymbol{r_E} + \boldsymbol{h}$, and $\boldsymbol{r_E}$ is the radius of the Earth at the location),** then the LT precession from the gravitomagnetic field ($\bar{H}$ at the foot of the previous slide) is given by,

$$\Omega_{LT} = \frac{G}{c^2 R^3} L' \left|1 - 3|\bar{z}.\bar{r}|\right|$$

The double modulus signs are needed to ensure that Ω_{LT} is always a positive angular precession, and the same values are obtained at numerically equal northern (+ve) and southern (-ve) latitudes.

[Cartmell, 2020; Cartmell, Faller, Lockerbie, Handous, 2020; Cartmell, Lockerbie, Faller, 2021]

Calculating the LT precession for the Foucault pendulum bob mass

The scalar angular momentum L' is given by $L' = I_{\oplus}\Omega_{\oplus}$ and considering the Earth initially as a non-oblate sphere, then $I_{\oplus} = \frac{2}{5}Mr_E{}^2$. But the actual radius of gyration of the Earth is 0.576 r_E, so the factor of $\frac{2}{5}$ becomes 0.576^2 which is 0.3316. Therefore $I_{\oplus} = 0.3316\, Mr_E{}^2$.

From which we obtain,

$$\Omega_{LT} = \frac{0.3316\, GM\Omega_{\oplus}}{c^2 R}\left|1 - 3|cos\theta|\right|$$

where $\bar{z} \cdot \bar{r} = cos\theta$ and $R \approx r_E$ for *h* very small indeed (assuming that the bob is hanging around a metre or so above the ground, for example). This result does not include the geodetic precession and is purely the LT component. The angle θ is the colatitude which is the included angle between $\bar{z}$ and $\bar{r}$ (the spin axis of Earth and the local vertical axis at the location, respectively) so $\theta = \frac{\pi}{2} - \phi$, where ϕ is the latitude as measured north or south from the equator.

Calculating the LT precession for the Foucault pendulum bob mass

Numerical data:

G = 6.67408*10^{-11} m^3 kg^{-1} s^{-2}

M = 5.972*10^{24} kg

$\Omega_\oplus$ = 7.2921150*10^{-5} rad/s

c = 2.99792488*10^8 m/s

R = 6356*10^3 m at the North Pole

R = 6363.18*10^3 m at Glasgow

ϕ = 1.5707963 rad at the North Pole

ϕ = 0.9750 rad at Glasgow

Numerical results

Using our result for LT precession we get $\boldsymbol{\Omega_{LT}}$ **= 219.5 mas/year** at the NP.

Pippard [Pippard, 1988] gives the LT precession as being **220 mas/year** at the NP. Ruggiero & Tartaglia [Ruggiero & Tartaglia, 2008] state the LT precession at the NP as **281 mas/year**.

By changing both the latitude and the radius of the Earth to the values for the location of Glasgow the LT can be calculated using our result on slide 16 to be $\boldsymbol{\Omega_{LT}}$ **= 162.6 mas/year**.

A new experiment – work in progress

Design specifications:

Pendulum fibre:

- The **longest possible fibre** compatible with the site.
- A wire made of fused quartz, fused silica, or sapphire, **coated with something conductive**, or semi-conductive like amorphous silicon. Alternatively, we could use high purity tungsten, but this is quite difficult material to transport and handle. No creep!
- We need **to minimise unwanted thermal stressing** and be aware of **exaggerated material brittleness due to cooling**, if applying heat shrink fitment.

Bob:

- The bob design will need to be **compatible with an electro-mechanical 'launcher'** mechanism needed for perfect take-off.
- **Compatible mechanically and electrically** with an electromagnetic pusher design (ref the ideas of Schumacher & Tarbet).
- The bob shape should be as dynamically close to a point mass as possible, so a squat cylinder is required, based on quadrupolar approximation to a sphere. Some test calculations show that a practical solution for this is quite possible **using tungsten or copper**.

Pendulum system design:

- An electro-mechanical launcher system is needed for perfect take-off. ★
- An electromagnetic 'pusher' system is needed to eliminate long-term ellipticity and to amplify and maintain swing motion. ☼
- A perfectly symmetrical upper pivot joint is required, with minimised frictional torque transfer from the rotating lab to the pendulum wire. ☼
- An aerodynamic enclosure is needed, together with a system for small pressure reduction inside the enclosure. ★
- Seismic isolation installation to minimise the transmission of seismic and man-made vibrations from the lab to the pendulum. ☼
- EMC protection to remove the effects of electrical and electromagnetic noise on the pendulum and its instrumentation. ☼
- A real time data-stream to determine the exact position of an external reference point, such as IM Pegasi (right ascension - 22 hours 53 minutes 2.27 seconds, declination - 16 degrees 50 minutes 28.3 seconds). ☼
- A bespoke laser tracking system to measure the precession of the pendulum relative to the lab to an accuracy of a few mas/year. ☼
- A system to measure local g to very high accuracy. ☼

The new experiment …

What is the resolution that we require for our instrumentation?

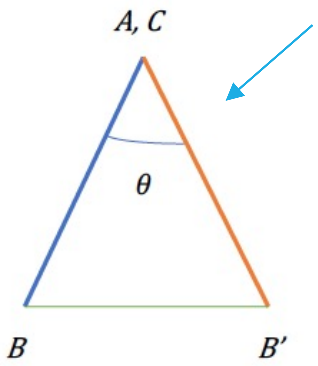

Looking down on plane CBB'

Our modelling predicts 162.6 mas/year for LT precession in Glasgow, Ω_{LT_G}. If we take an initial operation period of one year then geometry gives us $s = BB'$, so $\frac{s}{2a} = \sin\left(\frac{\theta}{2}\right)$, where 162.6 mas = 0.000045166°. If $a = 1$ metre then $s = 0.8\ \mu m$.

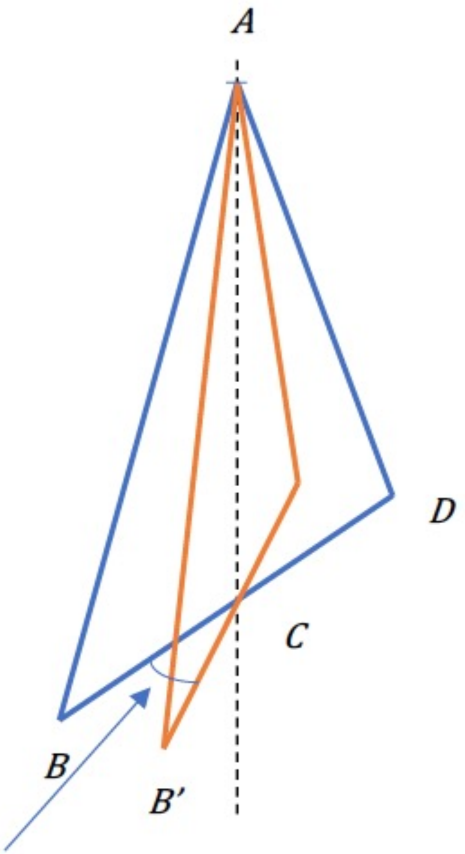

The LT measurement is simplest at the NP, where we have, $\Omega_{LT_{NP}} = \Omega_{FP_{m/E}} - \Omega_{gs/E}$, where $\Omega_{gs/E}$ is the apparent motion of a suitable guide star relative to the Earth, such as IM Pegasi. Elsewhere LT is modified by location both in terms of reduced FP precession and further corrections.

The angular velocity, $\dot{\theta}$ of the pendulum swing plane ABCD when it precesses round to AB'CD' is calculated to be 162.6 mas/year in Glasgow, Scotland.

The LT precession measured at co-latitude θ is given below (Braginsky, Polnarev, and Thorne, 1984) and comprises the measured precession of the pendulum bob *m* with respect to the Earth (first RHS term) minus the apparent precession associated with a guide star relative to the Earth (second RHS term) minus the precession of the pendulum relative to the guide star (third/fourth RHS term). At the poles the third/fourth terms go to zero because θ is zero at both poles. An urgent objective has been to calculate a typical numerical value for the third/fourth terms at the location of Glasgow to see how they might influence Ω_{LT_θ}.

$$\Omega_{LT_\theta} = \Omega_{FP_{m/E}} - \Omega_{gs/E} - \Omega_{\oplus}(1 - cos\,\theta)$$

The possible dominance of the third/fourth terms on Ω_{LT_θ} has to be determined as a priority. Significant variations in ϕ, hence θ arise because of fluctuations in local g, and this can be estimated by recourse to the WGS-84 local terrestrial gravity model which can be inverted to get ϕ from g_{local}.

WGS-84: $g_{local} = g_{eq}\left(\frac{1+k sin^2\phi}{\sqrt{1-\varepsilon^2 sin^2\phi}}\right)$ where $\varepsilon^2 = 1 - \left(\frac{b}{a}\right)^2$ and $k = \frac{(bg_p - ag_{eq})}{ag_{eq}}$

noting that $\theta = \frac{\pi}{2} - \phi$

g_{local} will be detected from a MEMS gravimeter as a continuous signal over time, and we can take g_{eq}, g_p, a, b as known values that can be input to a calculation based around the WGS-84 local terrestrial gravity model.

The gravimeter will give a fluctuating value for g_{local} over time, and this will have an upper and lower value, and a nominal value, with corresponding values for ϕ, which we define as, ϕ_U, ϕ_L, and ϕ_N, respectively. This means we can calculate three values for the co-latitude too, giving θ_U, θ_L, and θ_N. From that we can calculate three associated values of the right-hand-side third and fourth terms, as follows,

$$\Omega_{T_{3\&4}} = -\Omega_{\oplus}(1 - \cos\theta)$$

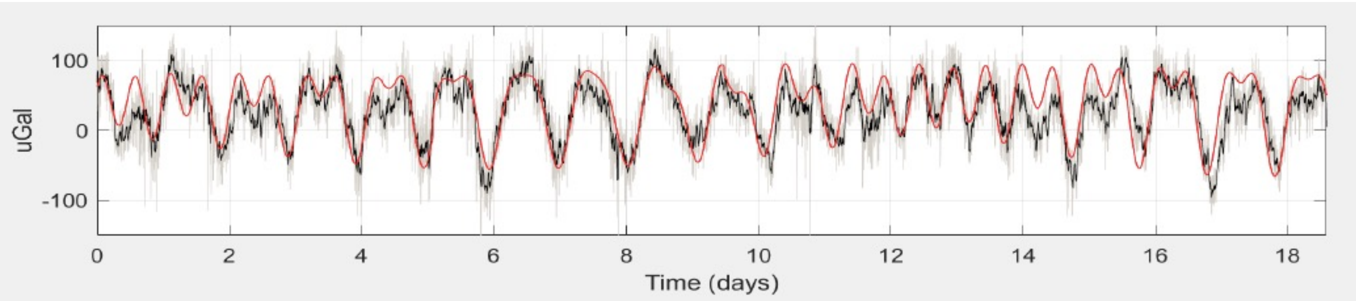

Measurement of fluctuations in the local gravitational acceleration in the city of Glasgow, Scotland, reproduced with the permission of the authors of *Microelectromechanical system gravimeters as a new tool for gravity imaging*. Phil Trans of the Royal Society A, 376, 20170291.

Range is $\pm 100\ \mu$gal $\equiv \pm$ 0.000001 m/s^2

The upper, lower, and nominal values of the third/fourth terms are,

$$\Omega_{T_{3\&4_U}} = -\Omega_{\oplus}(1 - \cos\theta_U)$$

$$\Omega_{T_{3\&4_L}} = -\Omega_{\oplus}(1 - \cos\theta_L)$$

$$\Omega_{T_{3\&4_N}} = -\Omega_{\oplus}(1 - \cos\theta_N)$$

g_{local_U}= 9.8156 + 0.000001 = 9.815601 m/s^2

g_{local_L}= 9.8156 – 0.000001 = 9.815599 m/s^2

g_{local_N} = 9.8156 m/s^2.

Using the WGS-84 model with free air correction for elevation of Glasgow at $h = 38$ m, we get the following latitude fluctuations:

$\phi_U = 0.973206$ rad/s, $\phi_L = 0.973165$ rad/s, $\phi_N = 0.973186$ rad/s.

Therefore,

$\theta_U = 0.597589$ rad/s, $\theta_L = 0.597631$ rad/s, $\theta_N = 0.597610$ rad/s.

Substituting the values for $\theta_U, \theta_L,$ and θ_N into the right-hand-side third and fourth terms gives:

$\Omega_{T_{3\&4_U}} = -0.0000126376$ rad/s, $\Omega_{T_{3\&4_L}} = -0.0000126393$ rad/s, $\Omega_{T_{3\&4_N}} =$
-0.0000126385 rad/s.

Converting these values from rad/s to mas/year requires a multiplicative conversion factor of 6.50477*10^{15} :

$\Omega_{T_{3\&4_U}} = -8.2204934323788848877 * 10^{10}$ mas/year

$\Omega_{T_{3\&4_L}} = -8.2216143848673263549 8 * 10^{10}$ mas/year

$\Omega_{T_{3\&4_N}} = -8.2210538999767593383 8 * 10^{10}$ mas/year.

The numerical range of the third and fourth right-hand-side terms shows how significant their contribution is to the measurement of LT precession, and this range is given by $\Omega_{T_{3\&4_U}} - \Omega_{T_{3\&4_L}}$, for which we get an absolute value (to five decimal places) of,

$\left|\Omega_{T_{3\&4_U}} - \Omega_{T_{3\&4_L}}\right| = 1.12095 * 10^{7}$ mas/year.

As we have seen, this range is due to a fluctuation in g_{local} = $\pm$ 100 μGal so these calculations confirm that these terms *will* dominate the measurement of LT. Results have also been obtained for g_{local} = $\pm$ 0 μGal, g_{local} = $\pm$ 50 μGal, g_{local} = $\pm$ 75 μGal, g_{local} = $\pm$ 125 μGal, and g_{local} = $\pm$ 150 μGal, and the values calculated for $Range_{T_{34}} = \left|\Omega_{T_{3\&4_U}} - \Omega_{T_{3\&4_L}}\right|$, and plotted on the graph shown next …

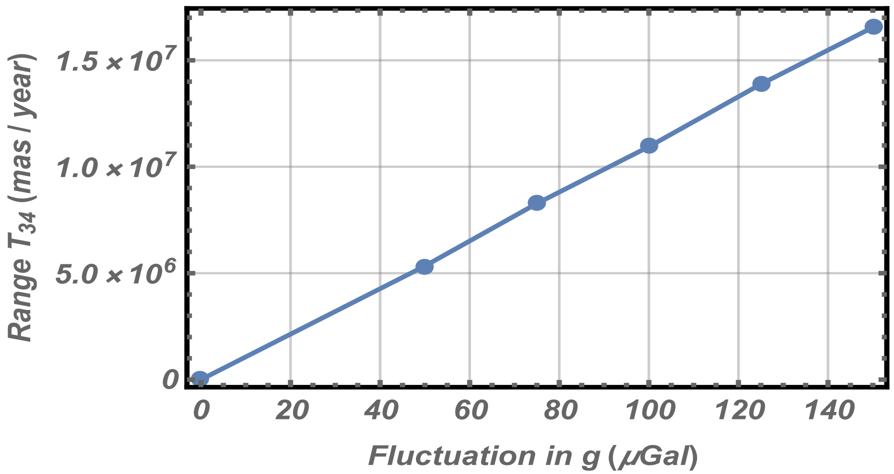

$Range_{T_{34}}$ as a function of $\pm$ peak fluctuations in the local gravitational acceleration in the city of Glasgow, Scotland.

Clearly the linear relationship in the Figure above confirms that the lower the measured fluctuation in g_{local} the lower the value of the range of terms T_{34}, and therefore the correspondingly reduced dominance of these terms within the measurement of Ω_{LT_θ}.

Confirmation of this finding is crucial for the data processing calculations that we are developing to ensure that the measurement of Ω_{LT_θ} is extracted to a very high level of fidelity.

Pendulum tracking geometry

Aim: the motion of the pendulum has to be measured in such a way that the extremely small component due to LT precession is detectable, and extracted unequivocally from the noise floor.

The primary requirement is for a non-contacting measurement system that can track the pendulum's motion continuously over time, and resolve the LT component.

High resolution cameras and autocollimators were considered but it was clear that in the case of the former the necessary resolution would only be available at extremely high cost, and the autocollimator option comes with a considerable additional complication in terms of the necessary tracking instrumentation and control. It is also noted that high quality industrial autocollimators are also extremely expensive.

It was decided to pursue a different approach in which an optical beam-crossing system using a small array of four laser line generators could be used to detect the presence of the pendulum bob. Sequential information extracted from this system could then be used then to infer the instantaneous position of the bob periodically, and then to use the time-base associated with the continuous sampling of that data to detect the small shifts in the timing of key points in the sequence, so to detect and quantify the LT precession.

We now proceed to summarise the three possible beam crossing geometries …

Case 1 – pendulum motion orthogonal to optical transmission path

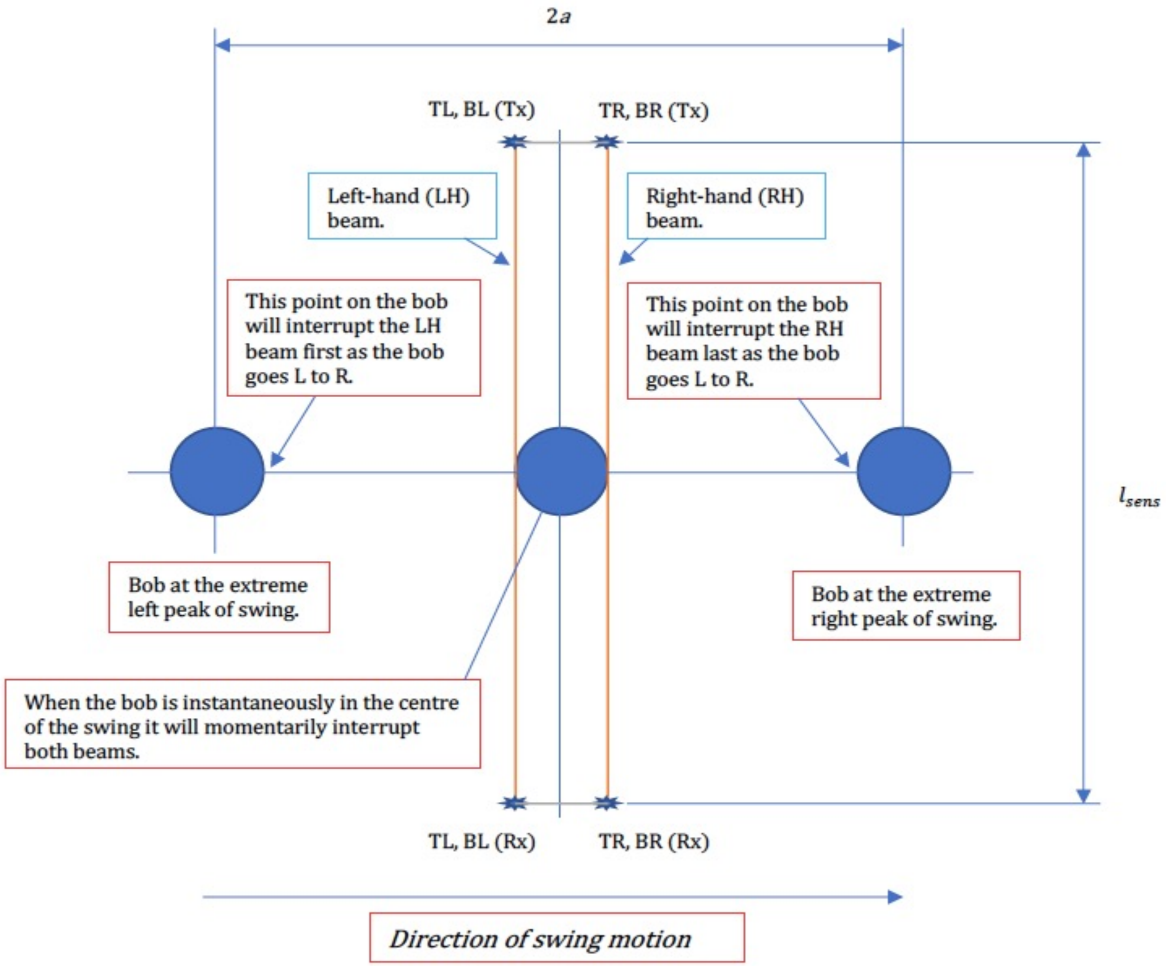

For this case the bob centre covers distance $2d_B$ from the instant the bob grazes the beam as it approaches, to the instant that it still (just) grazes the beam as it departs. So, the overall time in seconds taken from start to finish (of beam interruption) for this case is given by $2t_{d_B}$. Hence,

$$t_{2d_B} = \frac{d_B}{2af_n} = \frac{\pi d_B}{a\sqrt{\frac{g}{l_0}}}$$

Case 2 – pendulum swing plane located at an arbitrary angle of precession

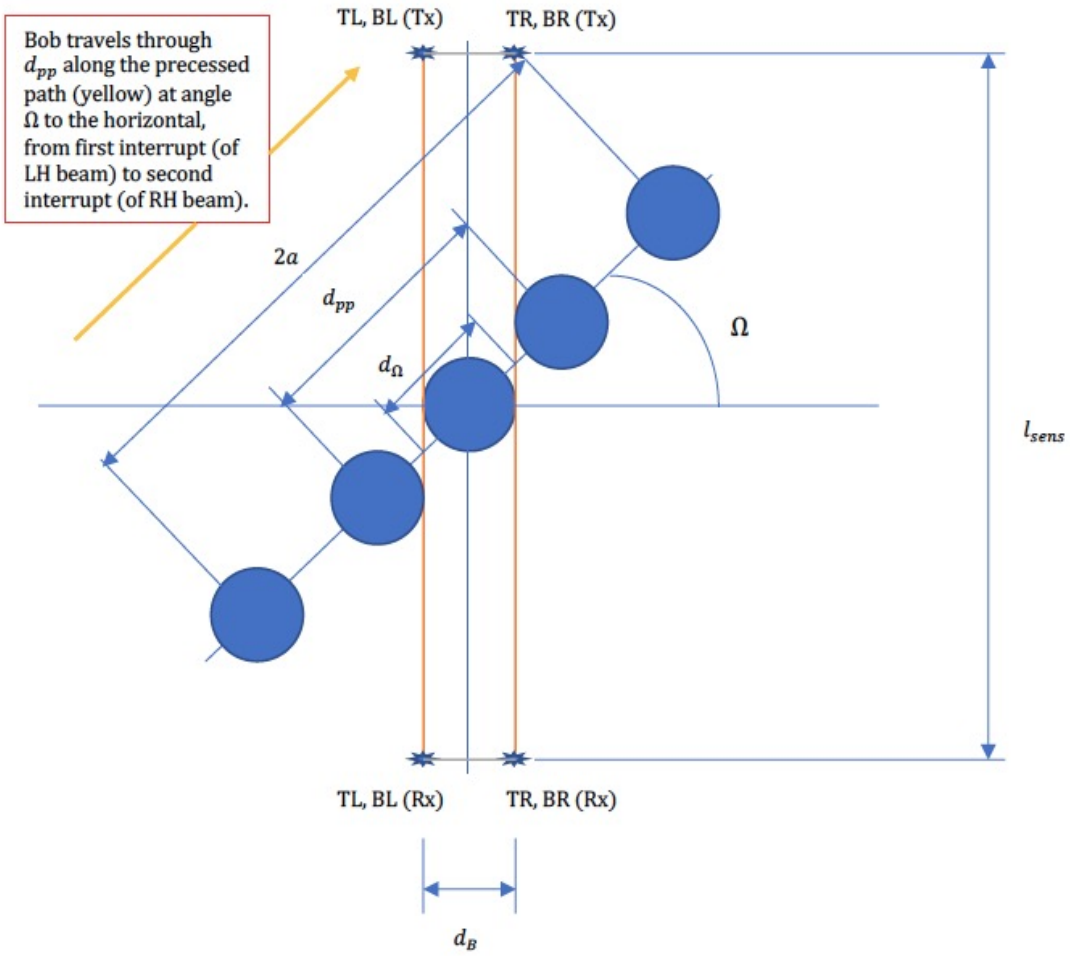

Here the pendulum has precessed through Ω so that the swing plane is no longer orthogonal to the optical transmission path, and instead is at an arbitrary precessional angle of Ω. So, the bob has to cover a longer distance d_{pp} to pass across the optical transmission path, and that distance is given by the following where Ω is in degrees,

$$d_{pp} = 2d_B + (2a - 3d_B)\frac{\Omega}{90}.$$

This means that the time to cover the TL, BL pair and then the TR, BR pair is a little longer than for the first case, and is found as follows,

$$t_{d_{pp}} = \frac{d_{pp}}{4af_n} = \frac{\pi\left(2d_B+(2a-3d_B)\frac{\Omega}{90}\right)}{2a\sqrt{\frac{g}{l_0}}}$$

sec, (where $t_{d_{pp}} < \frac{T}{2}$, and $\frac{T}{2} = \frac{1}{2f_n} = \frac{\pi}{\sqrt{\frac{g}{l_0}}}$).

Case 3 – pendulum swinging exactly along the optical transmission path

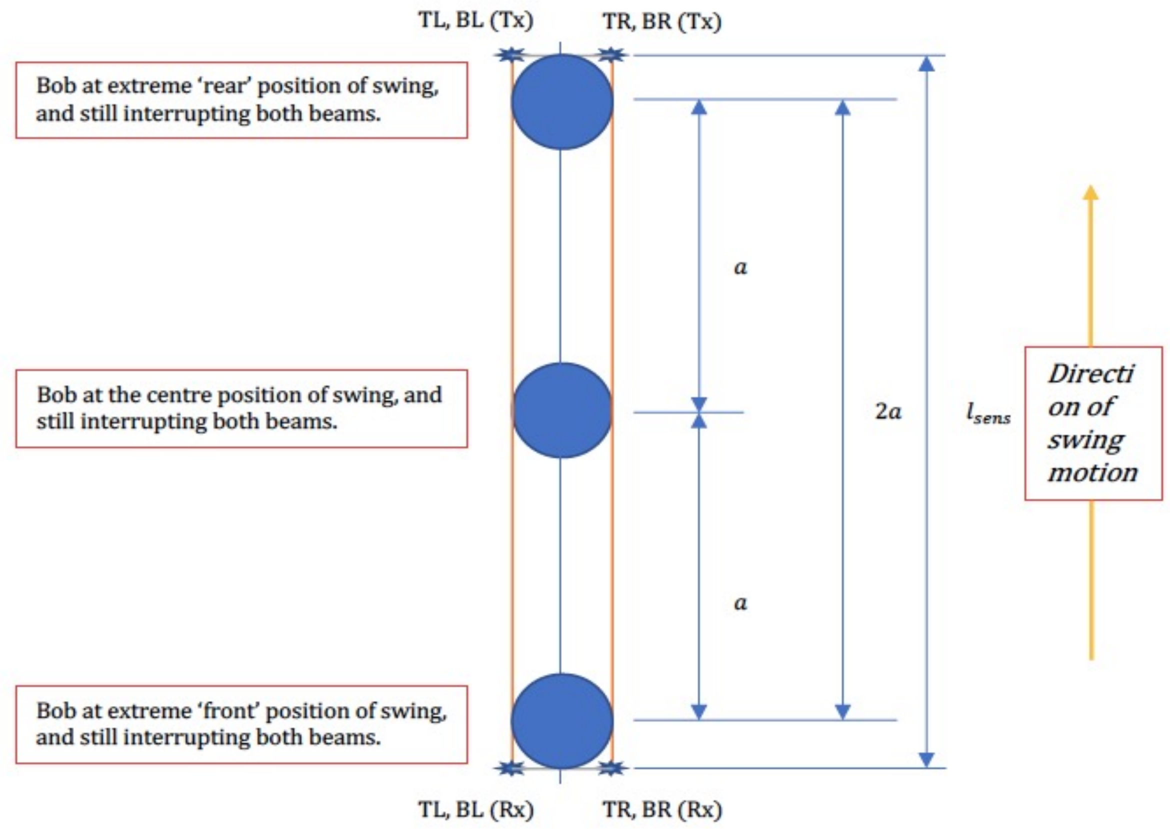

This simple case is shown in this Figure, in which both the beams are continually interrupted for the whole of the time that the swing plane of the pendulum is aligned with the optical transmission path. This is the case when $\Omega = 90°$. The time that the sensors are low over one half period is exactly equal to the half period itself. They will stay low for the remaining half period.

Ellipticity Control

The pendulum is only of any use as a measurement instrument for LT precession if it can be depended on to behave predictably over the long term. Unfortunately the performance of uncontrolled FPs is known to degenerate over time, particularly for shorter pendulum lengths.

We have already suggested that there are two practical solutions:

Principal parametric resonance (Pippard, 1988, Cartmell et al, 2021)

Forced excitation using phased electromagnetic pulses (Schumacher and Tarbet, 2020)

Extensive theoretical and practical tests of PPR show that it is highly effective in principle, both for ellipticity control and gain magnification, but the rise and fall of the pendulum bob due to length modulation makes any optical detection methodology extremely difficult to implement accurately.

The second approach has been investigated in detail for short FPs by Schumacher and Tarbet, 2020, and their results are reproduced with permission. This method for ellipticity control has been shown to be almost perfect, over long time-scales and is being adopted henceforth in this work. This system uses two concentric electromagnetic sensing and pusher coils to maintain planar motion of the pendulum after launch.

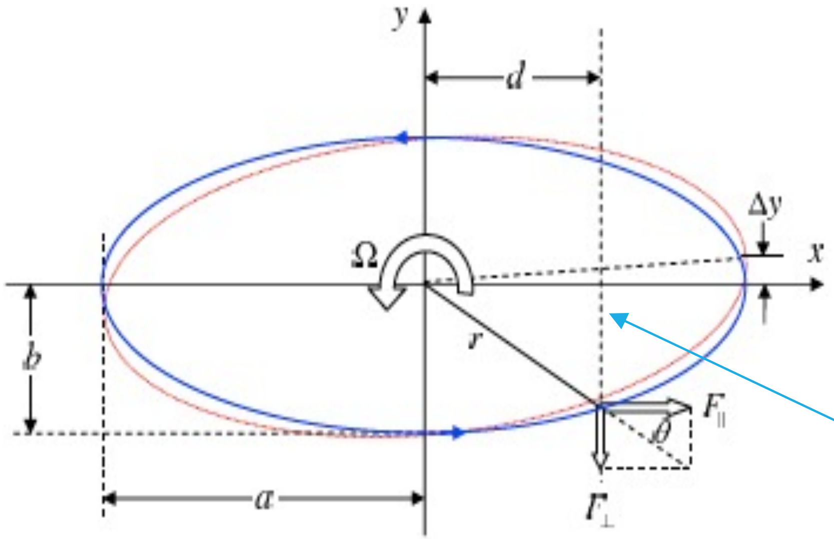

Vertical dotted line passing through point $(x_p, 0)$

The analysis of Schumacher & Tarbet, 2020, led to this result,

$$\frac{3}{4}\left(\frac{\pi\tau}{T}\right)\left(\frac{a}{l}\right)^2 = \frac{a}{d}\sqrt{1-\left(\frac{d}{a}\right)^2}\, cos^{-1}\frac{d}{a}$$

An algorithmic procedure then allows us to find drive pulse location $(^{d}/_{a})$ against drive pulse on-time t_d, to give really well maintained removal of ellipticity over time.

Figure and equation eproduced from Schumacher & Tarbet with the permission of the authors. The original caption stated: “Planar view of the approximate path of a spherical pendulum with semi-major axis *a* and semi-minor axis *b* that is moving in a counter-clockwise ellipse. The suspension is centred on the *z*-axis above the origin. The pendulum is precessing at rate Ω, and in one full cycle the apex advances by a distance Δy, as suggested by the light dotted and rotated ellipse. The impulsive driving force is applied at $x = d$, and it is resolved into components parallel and perpendicular at the major axis. The minor axis can be larger or smaller, resulting in a *b*-dependent magnitude of the transverse force $F_{\perp}$ for a fixed longitudinal force $F_{\parallel}$.”.

Electromagnetic excitation of the pendulum

Reproducing the equations of motion for the unforced pendulum and including the generalised forces Q_x and Q_y,

$$\ddot{x} + \eta|\dot{x}|\dot{x} - 2\dot{y}\Omega sin\phi - x\Omega^2 + \frac{gx}{l\sqrt{1 - \frac{x^2 + y^2}{l^2}}} = Q_x$$

$$\ddot{y} + \eta|\dot{y}|\dot{y} + 2\dot{x}\Omega sin\phi - y\Omega^2 sin^2\phi + r\Omega^2 sin\phi cos\phi + \frac{gy}{l\sqrt{1 - \frac{x^2 + y^2}{l^2}}} = Q_y.$$

The excitation system, based closely on the proposals of Schumacher & Tarbet, comprises two concentric coils with an outer sense coil and an inner exciter coil. The electromagnetic dipole force results from the interaction from a permanent neodymium magnet in the base of the bob and the inner exciter coil as the bob passes above. The exciter coil is driven by a high current low voltage supply which is pulsed electronically as the bob is detected by the outer sense coil, and so the form of the electromagnetic force pulse is broadly square, and in phase with the pendulum swing as the bob passes across the coils, noting that this is where the swing velocity is at a maximum.

The generalised forces are now,

$$Q_x = \frac{2}{\pi}\frac{F_{dip}}{M}\tan^{-1}\left(\frac{\dot{x}}{k}\right)\cos\left(\tan^{-1}\frac{y}{x}\right)$$

$$Q_y = \frac{2}{\pi}\frac{F_{dip}}{M}\tan^{-1}\left(\frac{\dot{y}}{k}\right)\sin\left(\tan^{-1}\frac{y}{x}\right)$$

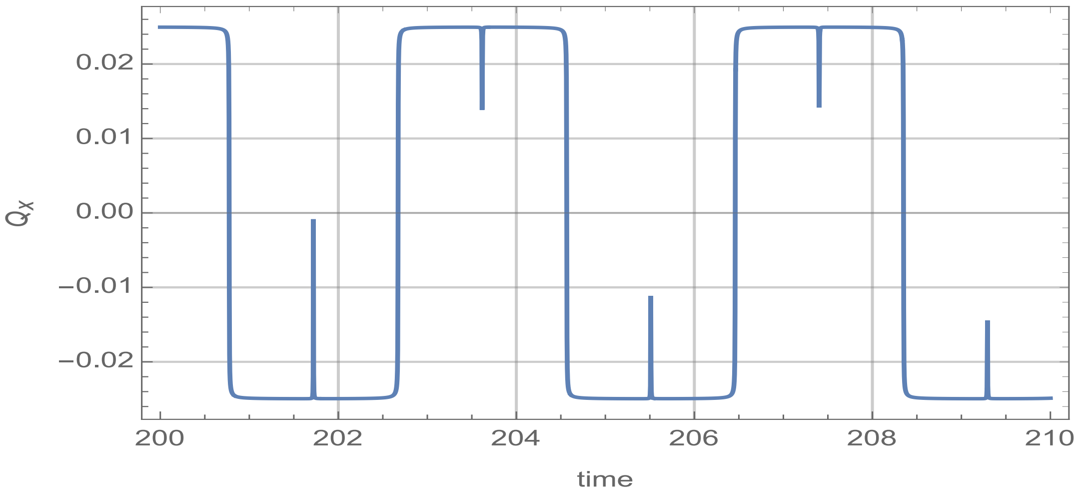

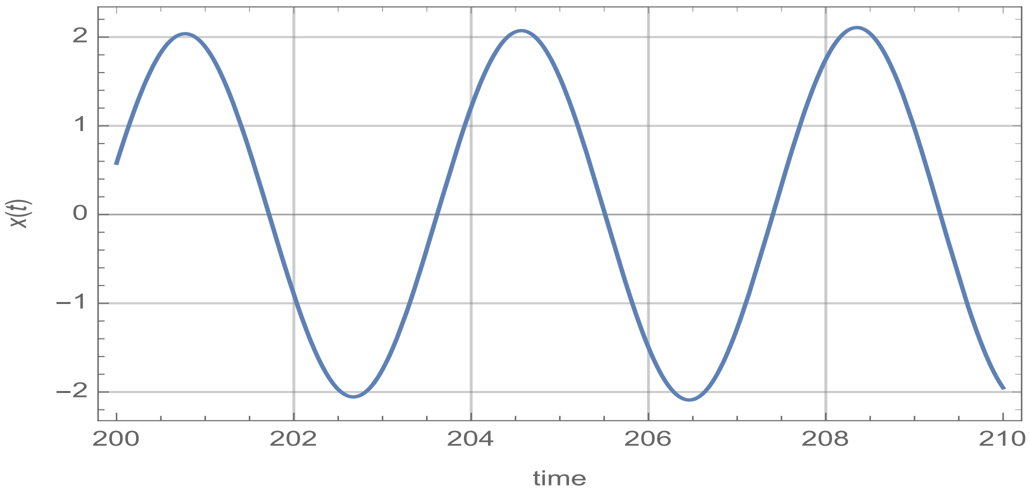

Upper plot: a snap-shot of the pulsatile generalised force Q_x (*N*) against time (*s*). **Lower plot**: a snap-shot of the response of the pendulum in x (*m*) against time (*s*).

The mid-point of the excitation pulse Q_x coincides with the zero-crossing of the pendulum in x where it reaches its maximum velocity.

Conclusions

1. We have derived a mathematical model of the dynamics of the Foucault pendulum and have validated it to within 0.1% using the North Pole as a reference location. This model is our basis for designing experimental pendulums.

2. Foucault pendulums are plagued by unwanted precessional effects, particularly as they get shorter in length. The most important of these effects is due to frequency anisotropy and generates an unwanted ellipticity in the response. We have a good practical solution to this based on the e/m pusher concept of Schumacher & Tarbet.

3. Frame-dragging is represented mathematically by Lense-Thirring precession. It is a fundamental phenomenon of gravity. There are several ways to calculate LT precession – we used GEM here to calculate a value for Glasgow, Scotland.

6. LT precession has been verified experimentally in LEO by two different space missions, but at very high cost.

7. We plan to try to measure it on Earth using a sensitive Foucault pendulum with very high resolution instrumentation. This is work in progress, with installation in a laboratory space at the University of Strathclyde scheduled to start on 6 December 2021.

8. The measurement is extremely difficult to make with any hope of accuracy, and the designs summarised here have to be supported by suitable signal processing algorithms – work currently in progress.

References

Wikipedia https://en.wikipedia.org/wiki/Foucault_pendulum (last accessed 7 October 2021)

Cartmell, M.P., Faller, J.E., Lockerbie, N.A., Handous, E.: On the modelling and testing of a laboratory-scale Foucault pendulum as a precursor for the design of a high-performance measurement instrument. Proc. R. Soc. A **476**, 20190680, pp. 26 (2020).

Pippard, A.B.: The parametrically maintained Foucault pendulum and its perturbations. Proc. R. Soc. A **420**, pp. 81-91 (1988).

Braginsky, V.B., Polnarev, A.G., Thorne, K.S.: Foucault pendulum at the South Pole: proposal for an experiment to detect the Earth's general relativistic gravitomagnetic field. Physical Review Letters, **53** (9), pp. 863-866 (1984)

Olsson, M.G.: The precessing spherical pendulum. Am. J. Phys. **46**, pp. 1118 (1978).

Plewes, D.B.: Magnetic monitoring of a small Foucault pendulum. Can. Rev. Sci. Instrument **89**, 065112 (2018).

Schumacher, R.A., Tarbet, B.: A short Foucault pendulum free of ellipsoidal precession. arXiv:0902.1829v2. (2009).

Chartas, G.: Frame Dragging, Department of Physics & Astronomy, College of Charleston, SC 29424, USA, http://chartasg.people.cofc.edu/chartas/Teaching.html (last accessed 7 October 2021).

Ciufolini, I., Dragging of inertial frames, Nature, 449, pp. 41–47 (2007).

Cartmell, M.P. Lense-Thirring precession – theoretical narrative, Research Report, University of Strathclyde, https://strathprints.strath.ac.uk/71740/ (last accessed 7 October 2021).

Ruggiero, M.L., Tartaglia, A., Gravitometric Effects, arXiv:gr-qc/0207065v2, (8 February 2008).

Acknowledgements

The author would like to thank the following people for their input to this project:

James E. Faller – for discussions of FP suspension point mechanics and FP design.

Eva Handous – for assistance with numerical experiments when designing the precursor test pendulum.

Nicholas A. Lockerbie – for discussions on the calculation of LT precession.

Reinhard A. Schumacher – for discussions on the e/m pusher concept and FPs in general

Kip S. Thorne – for discussions on the difficulties of measuring LT precession in non-polar terrestrial locations.

The accommodation provided for the new pendulum within the St. Pauls building, University of Strathclyde, is gratefully acknowledged.

Support funding for this research was obtained through the author's consultancy work during 2019 for the Advanced Forming Research Centre, University of Strathclyde, and this is acknowledged.